Electro-magnetic nano-particle bound Beclin1 siRNA crosses the blood-brain barrier to attenuate the inflammatory effects of HIV-1 infection *in vitro*

Myosotys Rodriguez[1], **Ajeet Kaushik**[1], **Jessica Lapierre**[1], **Seth M. Dever**[1], **Nazira El-Hage**[1,*], and **Madhavan Nair**[1]

[1]Department of Immunology, Florida International University, Herbert Wertheim College of Medicine, Miami, FL 33199, USA

Abstract

The purpose of this study was to evaluate a novel drug delivery system comprised of ferric-cobalt electro-magnetic nano-material ($CoFe_2O_4$@ $BaTiO_3$; MENP) bound to siRNA targeting Beclin1 (MENP-siBeclin1) to cross the blood-brain barrier (BBB) and attenuate the neurotoxic effects of HIV-1 infection in the central nervous system following on-demand release of siRNA using an *in vitro* primary human BBB model. Beclin1 is a key protein in the regulation of the autophagy pathway and we have recently demonstrated the importance of Beclin1 in regulating viral replication and viral-induced inflammation in HIV-1-infected microglia. The MENP-siBeclin1 nano-formulation did not compromise the physiological function or integrity of the BBB model. Furthermore, the *in vitro* BBB data revealed that MENP-siBeclin1 could efficiently attenuate viral replication, viral-induced inflammation and silence Beclin1 protein expression in HIV-1-infected microglial cells within the model system. In addition, the cytotoxic effects of direct treatment with siBeclin1 and MENP alone or in nano-formulation on primary human neuronal cells showed a minimal amount of cell death. Overall, the data shows that the nano-formulation can silence the *BECN1* gene as an effective mechanism to attenuate HIV-1 replication and viral-induced inflammation in the context of the BBB.

Keywords

magneto-electric nano-particles; RNA interference; autophagy; HIV-1; blood-brain barrier; neuro-inflammation

INTRODUCTION

Autophagy is a major catabolic pathway in which the cell degrades cytoplasmic contents through lysosomal fusion (Parzych and Klionsky, 2014). In our recent publication we showed that the use of small interfering (si) RNA targeting the *BECN1* gene (siBeclin1) can significantly reduce HIV-1 p24 levels and viral-induced release of inflammatory cytokines by infected microglial cells *in vitro* (El-Hage et al., 2015). Beclin1, the first mammalian

*Correspondence: Dr. Nazira El-Hage, Department of Immunology, Florida International University, Herbert Wertheim College of Medicine, Miami, FL 33199, USA; nelhage@fiu.edu; Phone: (305)-348-4878; FAX: (305)-348-1109.

autophagy protein to be described, has been well-characterized not only as an essential protein in regulating autophagic activity but also for its therapeutic potential in targeting diseases such as cancer (Fu et al., 2013, Kumar et al., 2015, Sun et al., 2015). Beclin1 can act as a positive regulator of autophagy and confers specificity to the phosphatidylinositol-3 kinase -Vps34-Atg14 complex, which is essential for autophagosome formation, and by interacting with the anti-apoptotic protein Bcl2, autophagy is inhibited (Parzych and Klionsky, 2014). In the last decade, numerous evidence has shown that autophagy is a critical target for HIV during the viral life cycle which has led to an increasing effort to understand the role of autophagy in those cells affected by HIV infection (Dinkins et al., 2015).

While there is still no cure for HIV/AIDS, a variety of anti-retroviral drugs that act on different stages of the HIV life cycle can be used in combination to control the virus (Nath and Steiner, 2014). However, despite the significant advances of cART (combined anti-retroviral therapy), the incidence of neurocognitive complications in the brain associated with HIV infection persists (Ene et al., 2011, Dahal et al., 2015), which partially results from the limited efficiency by which many of these drugs cross the blood-brain barrier (BBB) (Heaton et al., 2011, Atluri et al., 2015). Severe side effects, toxicities, compliance problems, and the emergence of drug-resistant strains further complicate the use of this therapy (Kaul et al., 2001, Wu et al., 2012). Microglia/macrophages are the predominant resident central nervous system (CNS) cell types productively infected by HIV-1. cART is not totally effective in controlling HIV-1 replication in microglial cells and does not directly target the inflammatory cascades which are believed to be the primary cause of neuronal injury or dysfunction related to HIV-associated dementia (HAD) pathology (Churchill et al., 2006, Lamers et al., 2010). Thus, there is an urgent need for innovative approaches in the treatment of HIV/AIDS, especially those targeting the root of inflammatory complications caused by the disease in the CNS.

In the last decade, the use of RNA interference (RNAi)-based therapeutics such as siRNA to mediate silencing of gene expression has shown exciting prospects for the development of novel therapeutic strategies (Ryther et al., 2005), including those for HIV infection (Novina et al., 2002, Lee et al., 2005, Rossi, 2006, Kumar et al., 2008). Despite the high potential utility of antisense therapy, its clinical application is limited mainly due to its short half-life *in vivo*, lack of target cell specificity, and poor transport across the cell membrane (Juliano et al., 1999). Furthermore, with brain being the target organ for HIV-associated neurocognitive disorders (HAND), it represents an additional impediment in the delivery of siRNA due to the presence of the BBB (Pardridge, 2007). However, the advent of nanotechnology has stimulated the development of innovative systems for the delivery of drugs and diagnostic agents to the brain (Suri et al., 2007). Magneto-electric nano-particles (MENPs) are a sub-group of multiferroic materials of about 20–40 nm in diameter possessing significant coupling ability of their magnetic and electric fields at physiological temperature (Nair et al., 2013). The movement of MENPs can be controlled for their effective penetration across the BBB by applying a relatively weak current of magnetic force (Nair et al., 2013). Here we have developed and evaluated the transport, on-demand delivery and efficacy of MENPs bound to siBeclin1 to target the effects of HIV-1 infection using an *in vitro* BBB model system comprised of infected microglia. The results demonstrate the

potential application of this innovative approach in attenuating the root of inflammatory complications leading to neurodegeneration caused by HIV-1 infection in the CNS.

MATERIALS AND METHODS

Cell culture

Commercially obtained primary human CNS cells (ScienCell Research Laboratories, Carlsbad, CA, USA), microglia (catalog #: 1900), neurons (catalog #: 1520), astrocytes (catalog #: 1800), brain microvascular endothelial cells (BMECs) (catalog #: 1710) and pericytes (catalog #: 1200), were cultured in their respective media as per the manufacturer's protocol.

HIV-1 infection of primary human microglial cells

Microglia were infected with HIV-1$_{SF162}$ (p24 = 1 ng/ml; from Dr. Jay Levy (Cheng-Mayer and Levy, 1988), obtained through the NIH AIDS Research and Reference Reagent Program (Germantown, MD, USA) as performed previously (El-Hage et al., 2013, El-Hage et al., 2014, El-Hage et al., 2015). HIV-1 infection was confirmed by quantification of p24 levels in culture supernatants using the RETRO-TEK HIV-1 p24 antigen ELISA kit (ZeptoMetrix, Buffalo, NY, USA) as performed previously (El-Hage et al., 2013, El-Hage et al., 2014, El-Hage et al., 2015).

In vitro blood-brain barrier (BBB) model

The BBB model was constructed by seeding different CNS cell types in a 24-well plate containing a transwell insert of 3 μm microporous semipermeable membrane. BMECs were grown to confluence on the upper (luminal) surface of the membrane immersed in their specific growth media and astrocytes and pericytes were grown on the bottom (apical) side of the membrane in close proximity to the BMECs. After the artificial BBB was formed in culture (5 days), the transwell insert was transferred into a 24-well plate containing HIV-1-infected microglia seeded at the bottom of each well (schematic presentation in Figure 1).

Preparation of CoFe$_2$O$_4$@BaTiO$_3$ magneto-electric nano-particles (MENPs) and time kinetics of MENP-Beclin1 siRNA nano-formulation

CoFe$_2$O$_4$@BaTiO$_3$ nano-particles were prepared according to the standard hydrothermal method as described previously (Kaushik et al., 2016). The average MENP shape and size of ~20 nm in diameter was determined using transmission electron microscopy (TEM) and the Scherrer equation, and the particle size distribution was measured using dynamic light scattering (DLS) technology from Malvern-Zetasizer instruments (Bennasser et al., 2007, Kaushik et al., 2016).

MENPs were dispersed in Tris-EDTA buffer (pH 7.4) and mixed with siBeclin1 in a 1:5 ratio solution containing a total of 2 μg siRNA and 10 μg MENP. Beclin1 siRNA was commercially purchased from Santa Cruz Biotechnology (Santa Cruz, CA, USA), catalog #: sc-29797 (El-Hage et al., 2015). The mixture was incubated in a tube rotator at room temperature and supernatant was collected after 60 minutes. The amount of bound siRNA or percentage binding to the MENP and the time kinetics of direct binding were measured by

absorption intensity of the siRNA at a wavelength of 268 nm using UV-Visible Spectroscopy (Hitachi U2910, Schaumburg, IL, USA).

Cell viability

Viability of microglia and neurons was assessed using a live/dead cell fluorescence assay which combines fluorescent reagents to yield two-color discrimination of the population of live cells indicated by green fluorescence from the dead-cell population indicated by red fluorescence (ScienCell Research Laboratories). Cells were imaged using an inverted fluorescence microscope (Zeiss, Germany) and viable cells were manually quantified and reported as percent of viability.

Physiological function of the BBB by Trans-endothelial Electrical Resistance (TEER) and immunocytochemistry

Electrical resistance across the BMEC monolayer of the artificial BBB model containing HIV-1-infected microglia was measured using a Millicell ERS microelectrode (Millipore, Bedford, MA, USA) as previously described (Ma et al, 1999; Haorah et al, 2005). The resulting TEER values were calculated minus the blank media control. Expression of occludin protein was detected by immunocytochemistry in BMECs grown to confluence on Lab-Tek tissue culture chamber slides (Thermo Scientific, Waltham, MA, USA) coated with polylysine (Thermo Scientific). Cells were fixed in 4 % paraformaldehyde, permeabilized with 0.5 % Triton X-100, blocked in 10 % milk/0.1 % goat serum, and immunolabeled. The antibody used was a monoclonal antibody against occludin conjugated to the Alexa Fluor 488 dye (catalog #: 331588; Thermo Scientific). DAPI staining was used to label cell nuclei and cells were imaged using an inverted fluorescence microscope (Zeiss).

ELISA

Microglial cell culture supernatants (pre-cleared by brief centrifugation) were used to measure the levels of interleukin (IL)-1, -6 and -8, monocyte chemotactic protein-1 (MCP-1), regulated on activation, normal T cell expressed and secreted (RANTES) and tumor necrosis factor alpha (TNF-α) by ELISA (R&D Systems, Minneapolis, MN, USA) according to the manufacturer's instructions. Culture supernatants containing HIV-1 particles were used to measure p24 protein levels by ELISA according to manufacturer's protocol (RETRO-TEK kit; ZeptoMetrix). The optical density (O.D.) was read at A450 on a Synergy HTX plate reader (BioTek).

Immunoblotting

Microglial whole cell lysates were prepared in RIPA buffer supplemented with a mixture of protease and phosphatase inhibitors and separated by SDS-PAGE for immunoblotting. Primary antibodies against Beclin1 (1:500), LC3-B (1:1000) and Lamp1 (1:100) were from Novus Biologicals (Littleton, CO, USA). Primary antibody against Atg 7 (1:200) was from Santa Cruz Biotechnology and GAPDH (1:1000) was from Sigma-Aldrich (St. Louis, MO, USA). Primary antibodies were followed by incubation with a secondary antibody conjugated to horseradish peroxidase (Cell Signaling Technology, Danvers, MA, USA) used at a 1:1000 dilution. Immunoblots were exposed to SuperSignal West Femto Substrate

(Thermo Scientific) and visualized using a ChemiDoc imaging system (Bio-Rad, Hercules, California, USA). Protein expression was calculated using ImageJ software (National Institutes of Health (NIH); Bethesda, MD, USA).

Acidic vesicle formation

Microglial cells were stained with 25 μg/ml acridine orange (AO) for 15 min. Cells were washed three times in phosphate-buffered saline (PBS), followed by examination under an inverted fluorescence microscope (Zeiss, Germany). The red/green fluorescence ratio for individual cells was calculated using ImageJ software (NIH).

Autophagy and NF-κB RT2 Profiler PCR Arrays

To elucidate a possible molecular mechanism in which silencing Beclin1 modulates HIV-1 infection and HIV-1-induced inflammation, autophagy and NF-κB-related gene expression in microglia was assessed following RNA isolation using the miRNeasy Mini Kit (Qiagen; Valencia, CA, USA). Purity of RNA was measured by a microspot RNA reader (Synergy HT Multi-Mode Microplate Reader from BioTek) and RNA preparations with an OD260 nm/ OD280 nm absorbance ratio of at least 2.0 were used for cDNA synthesis. One microgram of RNA was used for the first strand cDNA synthesis using Qiagen's RT2 First Strand Kit (catalog number #: 330401) as per the manufacturer's protocol. A genomic DNA elimination step was performed before reverse transcription. The relative abundance of each mRNA species targeted in the arrays was assessed by a RT2 SYBR Green/ROX PCR master mix (Qiagen; catalog #: 330520) containing 0.5 μg of RNA aliquoted in equal volumes (25 μl) into each well of the real-time PCR arrays using a Stratagene MX3000P (Santa Clara, CA, USA). The threshold cycle (Ct) of each gene was determined by using Stratagene MaxPro software. The threshold and baseline were set manually according to the manufacturer's instructions. Ct data were uploaded into the data analysis template on the manufacturer's website (http://pcrdataanalysis.sabiosciences.com/pcr/arrayanalysis.php). The relative expression of each gene was calculated using the   CT method with five housekeeping genes and compared with the expression in control cells.

Assessment of neuronal viability

Time-lapse digital images of neurons were recorded using an inverted microscope with an automated computer-controlled stage encoder and environmental chamber (37 °C, 95% humidity, 5% CO_2) (Zeiss) that allowed repeated tracking of individual neurons per treatment over time. Neuronal death was considered to have occurred upon collapse and fragmentation of the cell body.

Statistical analysis

Data were analyzed using analysis of variance (ANOVA) techniques followed by Bonferonni's post hoc test for multiple comparisons (GraphPad Prism 6 software, La Jolla, CA, USA). A value of $p < 0.05$ was considered significant.

RESULTS

Artificial blood-brain barrier (BBB) model system and strategy for MENP-siBeclin1 nano-formulation transmigration

The particle size and topology of synthesized $CoFe_2O_4@BaTiO_3$ nano-particles were characterized using transmission electron microscopy (TEM) (Fig. 1A). The average size of ~20 nm in diameter was determined using previously reported methods. The difference between the total siRNA added and unbound siRNA was used to calculate the amount of siRNA bound to the MENPs and showed a binding efficiency of 50% detected at 10 minutes which was steadily increased with time. A maximum binding of 90% was achieved after 30 minutes of incubation (Fig. 1B). A schematic representation of the nano-formulation is shown in Fig. 1C. To begin to evaluate the functional effects of the nano-formulation in the context of the BBB, an artificial BBB was first constructed in culture using primary human CNS cell types. For all experimental treatments a 50 μL volume of media containing (i) siBeclin1 (2 μg), (ii) MENP (10 μg) or (iii) siBeclin1-MENP (in a 1:5 ratio concentration) was added to the artificial BBB construct containing HIV-1-infected microglial cells at the bottom chamber of the model (Fig. 1D). Two different kinds of magnetic fields were applied to the plate (Fig. 1E–F). Both magnetic fields are of a different nature and have different roles in respect to the delivery of the nano-formulation and release of the siRNA. A static magnetic field that doesn't change the polarization of the nanoparticle was applied first at 0.8T for a duration of 3 hours in order to transmigrate the nano-formulation across the blood-brain barrier model (Fig. 1E–F). Secondly, an alternating current (a.c) magnetic field (60 Oersted, at 1000 Hz frequency) was applied externally via electromagnetic coils to the plate for 30 minutes in order to release the siBeclin1 from the MENP surface area (Fig. 1G). AC based magnetic field changes the polarization of the nano-formulation and thus used in the release of the siRNA. A duration of 3 hours is based on an optimized exposure time (Kaushik et al., 2016) to achieve maximum nano-formulation delivery and 30 minutes is based on an optimized exposure time to achieve maximum siRNA release. Using an iron-based assay (Jayant et al., 2015), the amount of MENP transmigrated through the BBB after 3 hours was calculated to be approximately 30%, and using the optical density (O.D.) (Fig. 1B), it was estimated that ~0.7 μg of siBeclin1 transmigrated via the MENP (Fig. 1G). After different time points as indicated in the text, the transwell insert containing the BBB was removed, and supernatants and cell lysates from the bottom chamber of the BBB were collected and stored at −80 °C for later use.

Nano-bound Beclin1 siRNA does not compromise the physiological function of the BBB model

We first determined whether transmigration of the nano-formulation could lead to disruption of the BBB. The integrity of endothelial tight junctions in the artificial BBB was measured by Trans-endothelial Electrical Resistance (TEER) at time 0 and at 3 and 24 hours post-treatment. The results showed TEER values of around 190–200 Ωxcm^2 at each time point, indicating that the electro-magnetic forces and MENP migration did not alter the integrity of the BBB under the different treatment conditions (Fig. 2A). Even after 24 hours of treatment no significant differences between siBeclin1 and MENP alone or combined as a nano-

formulation were detected, suggesting that the siRNA nor the MENP were inherently toxic to endothelial cells even after an extended time point of treatment (Fig. 2A).

We next assessed whether the different treatment conditions could alter expression levels of the tight junction protein occludin using immunocytochemistry. The results showed no visible differences in the amount of occludin immunoreactivity with siBeclin-MENP when compared to media control, siRNA or MENP alone treated endothelial cells in the HIV-1-infected artificial BBB model indicating that tight junction protein expression was not compromised by the nano-formulation (Fig. 2B).

Nano-bound Beclin1 siRNA crosses the BBB model to attenuate HIV-1 replication and viral-induced inflammation

Next, we evaluated the efficacy of the nano-formulation to attenuate viral replication and induced inflammatory responses in microglial cells as part of the artificial BBB model. At the indicated time points following transmigration and siRNA release, the transwell insert containing the artificial BBB was removed and supernatant from the HIV-1-infected microglial cells seeded at the bottom chamber was collected. Viral titer as measured by HIV-1 p24^{gag} protein ELISA was significantly decreased in the supernatant of cells treated with the MENP-siBeclin1 nano-formulation compared to the other treatment groups (Fig. 3A–B). In fact, viral titer was reduced by $53.6 \pm 1.2\%$ after 24 hours (Fig. 3A) and by $30.3 \pm 1.8\%$ after 48 hours (Fig. 3B) post-treatment when compared to HIV-1-infected cells alone. Of note, siBeclin1 alone did not cause a significant decrease in viral titer, suggesting that in an unbound state the siRNA is not as stable and easily degraded or naked siRNA does not enter cells as effectively as when bound to a nanoparticle. Also, the reduced reduction in viral titer that we observed at 48 hours when compared to 24 hours suggests that the activity of the nano-formulation decreases within this time frame (Fig. 3A–B).

Since inflammation plays an important role in the neuropathogenesis of HIV-1, we measured levels of pro-inflammatory cytokines and chemokines by ELISA (Fig. 3A–B). Twenty-four hours post-treatment with the nano-formulation caused a significant decrease in the release of MCP-1 ($44.3 \pm 0.9\%$), IL-8 ($22.6 \pm 0.2\%$), TNF-α ($32.6 \pm 0.3\%$), RANTES ($25.9 \pm 0.5\%$) and IL-6 ($40.7 \pm 0.4\%$) when compared to all other groups (Fig. 3A). Significant decreases in the secretion of MCP-1 ($32.4 \pm 0.4\%$), IL-6 ($37.9 \pm 0.3\%$) and IL-8 ($10.3 \pm 0.5\%$) were also detected after 48 hours post-treatment (Fig. 3B), suggesting that depending on the cytokine the effect of the nano-formulation can have more of a sustained rather than transient response. Collectively, the attenuation of viral titer correlates with an inhibition in the release of cytokines and chemokines. Most importantly, the data suggest that the nano-formulation can efficiently cross the BBB, and on-demand release of siRNA as determined by the effective attenuation of viral replication and viral-induced inflammation in microglial cells is a good indication of the functional efficiency and stability of this nano-formulation. Furthermore, since no inhibitory effect was detected with MENP alone, this further confirms that the functional effects detected were due to the transmigration and release of siRNA.

Nano-bound Beclin1 siRNA crosses the BBB model to down-regulate Beclin1 protein expression levels and affect autophagy in HIV-1-infected microglial cells

We next determined whether the differences detected above were in fact due to decreases or imbalances in the autophagy pathway expected from Beclin1 silencing. Lysates from HIV-1-infected microglial cells were analyzed by western blotting and showed a significant down-regulation of Beclin1 protein expression levels after 24 and 48 hours post-treatment with the nano-formulation (Fig. 4A–B). Down-regulation of Beclin1 protein was also detected in lysates from cells treated with siBeclin1 alone for 24 hours (Fig. 4A), and although the decrease was significantly different from the control treatment, the suppression was significantly less than that of the nano-formulation, suggesting that siRNA in the complex of the nano-formulation is more stable and effective. Down-regulation of Beclin1 after 24 and 48 hours may have caused a slight dysregulation in autophagy as detected by decreases in the protein levels of LC3-B and Atg7 (Fig. 4A–B). Furthermore, several studies have reported that nanoparticles can accumulate inside lysosomes and acidic vesicles, causing intracellular acidification and an increase in autophagy (Stern, 2008; Neun, 2010; Stern, 2012). With this in mind, we measured levels of the lysosomal-associated membrane protein (Lamp) 1 and detected increased protein expression in lysates from cells treated with the nano-formulation at 24 hours and both MENP and nano-formulation at 24 and 48 hours (Fig. 4A–B), suggesting that high amounts of lysosomes were present when treatment with MENPs. Collectively, the data suggest that on-demand release of siRNA from the nano-formulation across the BBB results in effective Beclin1 silencing to attenuate viral replication and viral-induced inflammation in microglial cells by disruption of the autophagy pathway.

Nano-bound Beclin1 siRNA does not compromise the viability of microglial cells

To determine whether the functional effects of the nano-formulation can lead to cell death, microglial viability was assessed after 24 and 48 hours post-treatment using a live/dead cell assay (Fig. 5). No significant differences were observed in the viability of HIV-1-infected or un-infected microglial cells under the different treatment conditions (Fig. 5A). Based on the increased LAMP1 expression levels (Fig. 4A–B), we also determined whether the nano-formulation could change vesicular pH (Fig. 5B–C). AO is a fluorescent weak base that accumulates in acidic compartments and emits a red fluorescent signal that can be used to visualize lysosomes and evaluate gross abnormalities in lysosomal pH. MENPs alone or in nano-formulation did not cause a significant shift in pH as detected by the formation of red punctae (Fig. 5B–C), suggesting that increased Lamp 1 expression in microglial cells treated with the MENP alone or as bound nano-formulation (detected in Fig. 4A–B) is not attributed to increased vesicular acidification.

Down-regulation of NF-κB and autophagy related genes by siBeclin1

NF-κB-related signaling has long been considered a prototypical pro-inflammatory pathway (Pitha, 2011, Fiume et al., 2012). Therefore, we explored this as a possible signaling pathway by which siBeclin1 attenuated the release of inflammatory molecules from HIV-1-infected microglial cells. Out of 84 key genes related to NF-κB-mediated signal transduction, HIV-1 significantly induced the expression of the inflammatory chemokine

IL-8, the Signal Transducers and Activators of Transcription, STAT1, and Akt1, while siBeclin1 caused a down-regulation in HIV-1-induced expression of those genes (Fig. 6A). Of note is that the expression of several other genes were either up- or down-regulated by HIV-1, however, since the expression of these genes were not affected by siBeclin1 they were not considered to be mediated by the autophagy pathway and not mentioned (6B). In addition, we further determine whether additional autophagy related genes converge with this pathway. Out of 84 autophagy related genes interrogated, HIV-1 increased *BECN1, ATG16L1, ATG16L2, GABARAPL2, GABARAPL1, ATG3, IGF1* and *MAP1LC3A* gene expression when compared to untreated control cells, while silencing with siBeclin1 decreased the HIV-1-induced expression levels of these genes (Fig. 6A). The genes for GABARAP and GABARAPL1 are subfamilies of MAP1LC3 and homologues of Atg8, which are all involved in elongation of the phagophore and formation of autophagosomes; however, the GABARAP subfamily is essential for a later stage of autophagosome maturation (Shpilka et al., 2011).

Nano-bound Beclin1 siRNA does not compromise the viability of neurons

Since the ultimate goal of developing the nano-formulation is for it to be used in an environment that contains neurons, we next determined the effect of the nano-formulation on neuronal viability for up to 72 hours exposure. Tracking individual neuronal cell death using time-lapse imaging revealed that treatment with nano-bound Beclin1 siRNA did not cause significant toxicity to neurons throughout the treatment period when compared with media only control and the other treatment groups (Fig. 7A). At the end of the time-lapse experiments, neuronal viability was confirmed by a fluorescent live/dead cell assay. As seen for the time-lapse analysis, MENP-siBeclin1 did not exert significant neuronal death at 72 hours of exposure when compared with the other groups (Fig. 7B–C).

DISCUSSION

Although several studies have suggested the use of nanoparticles to deliver anti-retroviral drugs to the brain (Nair et al., 2013, Fiandra et al., 2015, Jayant et al., 2015), there is still an urgent need to apply this technology to target prevalent HIV-1-induced inflammation. In this study we used a non-toxic, on-demand delivery method developed and optimized by Kaushik et al. (Kaushik et al., 2016) to bind and transport siBeclin1 through an artificial BBB. Concurring with the Kaushik study, our *in vitro* data demonstrated that MENPs alone do not affect cellular viability. More importantly, we demonstrated that nano-bound Beclin1 siRNA does not compromise the physiological integrity of the BBB *in vitro* and does not affect individual cell type viability. TEM imaging and OD measurements of the bottom chamber of the artificial BBB confirmed that nano-bound Beclin1 siRNA efficiently crossed the artificial BBB with significant amounts and deposited with minimal agglomeration through the microglial monolayer (Fig. 1). Upon delivery to the bottom chamber, nano-bound Beclin1 siRNA did not significantly alter microglial morphology or viability. Even though we found nano-bound siBeclin1 did not exert any direct toxicity, several studies have reported that nanoparticles can accumulate inside lysosomes and acidic vesicles, causing intracellular acidification and an increase in autophagy (Stern and Johnson, 2008, Neun and Stern, 2011, Stern et al., 2012). These findings by others prompted us to analyze expression

of the lysosomal membrane protein Lamp1 in HIV-1-infected microglial cells treated with MENPs alone or as a nano-formulation (Fig. 4). While we did observe increased expression of Lamp1 in MENP-siBeclin1-treated cells, the up-regulation was not necessary a consequence of an increase in acidic vesicle formation or acidification as detected by acridine orange staining (Fig. 5).

After finding that nano-bound Beclin1 siRNA efficiently crossed the artificial BBB without altering cellular viability, we then determined whether the nano-formulation was able to attenuate viral replication and the release of inflammatory molecules from HIV-1-infected microglial cells as part of the model system. We showed nano-bound Beclin1 siRNA significantly decreased p24 levels in microglial supernatant after 24 hours of treatment and that this viral reduction was still sustained after 48 hours. Moreover, since the release of inflammatory molecules plays a key role in HIV-1-induced neuropathogenesis (Kaul et al., 2001, Wang et al., 2003, Nolting et al., 2009, Hazleton et al., 2010), we further examined whether nano-bound Beclin1 siRNA could also modulate cytokine and chemokine release by infected microglia. Twenty-four hours of treatment with nano-bound Beclin1 siRNA caused significant decreases in IL-8, IL-6, RANTES, MCP-1 and TNF-α. More importantly, after 48 hours of treatment IL-6 and MCP-1 which are known to be principal inflammatory molecules in HIV-1-induced neuroinflammation (Eugenin et al., 2006, El-Hage et al., 2008, Airoldi et al., 2012) remained decreased. Taken together, we report that nano-bound Beclin1 siRNA not only effectively decreases HIV-1 replication but it also maintains decreased levels of inflammatory molecules in HIV-1-infected microglia. It is important to note that this reduction is not likely due to direct cellular toxicity.

These observations correlate with several studies reporting that inhibition of autophagy results in attenuation of microglial-driven inflammation (Deretic et al., 2013, El-Hage et al., 2015, Guo et al., 2015). Of note is that we previously did not observe a significant decrease in IL-8 release when blocking the autophagy pathway with siBeclin1 (El-Hage et al., 2015). The discrepancies between the two studies may be due to differences in several experimental parameters. In the present study, we assessed the possibility of using siBeclin1 as a potential therapeutic strategy for targeting HIV-1-related neuropathology and infected the human microglial cells first with HIV-1 followed by transfection with siBeclin1, while in the previous study we explored whether autophagy is an essential mechanism through which HIV-1 replication is mediated and thus cells were transfected first followed by infection. Secondly, the duration of treatment was different. In the present study the release of inflammatory molecules was measured after 24 and 48 hours, versus 24 hours only (El-Hage et al., 2015). Cytokine and chemokine release patterns can greatly differ depending on the stimulus, sequence of treatments and time of sample collection (Graziosi et al., 1996, Fan et al., 1998, Minogue et al., 2012).

In general, it is well accepted that NF-κB activation is one of the principal pathways that induce expression of inflammatory molecules in microglia (Wang et al., 2012, Park et al., 2013). Interestingly, increasing evidence suggests the NF-κB pathway as a possible mechanism in which inhibition of autophagy results in attenuation of inflammatory responses (Jiang et al., 2012, Deretic et al., 2013). With this in mind, we assessed whether nano-bound Beclin1 siRNA decreases cytokine and chemokine release through modulation

of the NF-κB pathway. NF-κB array results from total mRNA showed that silencing Beclin1 with siRNA in the context of HIV-1 infection decreased several NF-κB-related genes when compared to HIV-1 infection alone (Fig. 6). Another factor to take into consideration is that both autophagy and NF-κB pathways are interlinked cellular processes, essential for cell survival (Qing et al., 2007, Kang et al., 2011). The IκB kinase (IKK) subunit of the NF-κB pathway, which has been shown to act as a tumor suppressor, effectively activates autophagy through Beclin1 interactions (Criollo et al., 2010). Interestingly, we did not detect a significant difference in IKK gene expression when silencing Beclin1. Furthermore, expression of IL-8 protein (Fig. 3) and mRNA (Fig. 6) was decreased with siBeclin1, probably due to the down-regulation of STAT1 activity (Fig. 6). STAT1 plays vital roles in signaling pathways that regulate the immune response, and studies by others have shown regulation of IL-8 production through STAT1 rather than NF-κB (Chaudhuri et al., 2008, Yang et al., 2009). Moreover, others have shown that there is a high predominance of spontaneous tumors and decreased autophagy in Beclin1−/− mutant mice (Yue et al., 2003). Although siBeclin1 caused an increase in the proto-oncogene c-MYC, and 2-fold decrease in the anti-apoptotic gene Bcl2, we did not observe a significant effect on cell viability, cell morphological changes or an increase in other apoptotic markers. The correlation between the NF-κB and autophagy pathways is of a complex nature and ongoing studies in the lab will aim to further elucidate this connection and the effect on cell survival. The delivery efficiency of the nano-formulation through the *in vitro* BBB model was attested by the attenuation of HIV-1 replication and viral-induced inflammation, which was followed up by assessing if the response of nano-formulation was in fact due to the expected downregulation of Beclin1 protein expression levels. We detected a significant decrease in Beclin1 protein after treating with nano-bound Beclin1 siRNA for 24 hours. This result confirms that nano-bound Beclin1 siRNA stability and activity still remained after crossing the artificial BBB. Among the key mediators initiating autophagosome formation, there is a set of evolutionarily conserved autophagy-related gene products including the Class III phosphatidylinositol 3-kinase (Class III PI3K) complex (composed of Beclin1/Atg6-hVps34, hVps15 and Atg14L) (Kang et al., 2011). The Levine group has extensively demonstrated that Beclin1/PI3K complexes may not only function in autophagosome formation, but also in autophagosome/endosome maturation (He and Levine, 2010). By recruiting different binding partners and forming distinct PI3K-III complexes, Beclin1 modulates PI3K-III activity and thus regulates autophagy at multiple stages including nucleation and maturation (McKnight and Zhenyu, 2013). Therefore, Beclin1 and PI3K interactions have been contemplated as a possible target for autophagy modulation. In this study, we did not see a modulation on PI3K-III when silencing Beclin1, however, AKT1gene expression was down-regulated. Because PI3K/AKT/mTOR pathway is an essential survival pathway (Li et al., 2016), it is important to cautiously monitor this pathway. Although AKT1 levels were lowered, we did not observe a significant effect on cell viability, cell morphological changes or an increase in other apoptotic markers. In terms of other autophagy-related proteins, silencing of Beclin1 by nano-bound Beclin1 siRNA coincided with a down-regulation in LC3-B and Atg7 protein expression. Since LC3-B is present in the autophagosomes are degraded after fusion with lysosomes, the observed decrease in this protein may suggest that nano-bound Beclin1 siRNA modulates early steps of the autophagy pathway (Mizushima et al., 2010). Thus, our results imply that down-

regulation of Beclin1 causes imbalances in the autophagy pathway. Most importantly, the significant decrease in Beclin1 protein expression was maintained after 48 hours of nano-bound Beclin1 siRNA treatment.

Another important aspect to be considered with the application of this technology is the effect of autophagy modulation on different CNS cell types. Several studies have reported that deficits in autophagy could lead to more rapid neurodegeneration (Alirezaei et al., 2008, Fields et al., 2013). Moreover, sustained silencing of the autophagy pathway could result in cell damage, although this was not detected in our system. Autophagy-induced cell death is a controversial topic as shown by some that inhibition of autophagy leads to cell death by an increase in apoptosis while others have shown autophagy as a cell survival mechanism (Eskelinen, 2005, Liu and Levine, 2015). Our future goal is aimed to achieve viral silencing leading to inhibition of viral production in the central nervous system. The siBeclin1 nano-formulation will be encapsulated in biodegradable liposomes containing surface antibody markers specific to microglial cells that will directly target HIV-1-infected and activated microglia in the central nervous system, an environment that contains neuronal cells. Thus, in assessing viability of all cellular components of our in vitro BBB model, we also determined whether nano-bound Beclin1 siRNA would exert any direct toxicity to neurons (Fig. 7). Time-lapse imaging data showed that nano-bound Beclin1 siRNA did not exert significant direct toxicity to neurons and theoretically can be used effectively in an environment containing different neuronal cell types. Despite the promising features of using this magneto-electric nanotechnology approach, there are still several limitations to achieving effective delivery and functionality *in vivo* (Begley, 2004, Wohlfart et al., 2012), including the ability of carriers to overcome the BBB and produce biologic effects in the CNS. There are several parameters one has to take into consideration including the choice of proper biodegradable material for nanoparticle preparation, the efficiency of drug loading and the drug release pattern, the size and stability of the particle and other safety issues. Ongoing studies will assess whether siBeclin1 bound to MENPs can be systemically delivered effectively to the brain in *in vivo* models such as mice.

In summary, herein we show proof-of-concept that decreasing Beclin1 expression by delivery of siRNA using nano-particles can attenuate HIV-1 replication and viral-induced cytokine and chemokine release through transmigration of an *in vitro* BBB without illicit toxicity to brain cells. This study shows for the first time a novel approach using on-demand delivery of silencing autophagy as a potential therapeutic intervention to attenuate the neurodegenerative effects of HIV-1 infection in microglial cells. The next logical step is to determine if our novel nano-formulation can be delivered safely and effectively *in vivo*.

Acknowledgments

References

Airoldi M, Bandera A, Trabattoni D, Tagliabue B, Arosio B, Soria A, Rainone V, Lapadula G, Annoni G, Clerici M, Gori A. Neurocognitive impairment in HIV-infected naive patients with advanced

disease: the role of virus and intrathecal immune activation. Clinical & developmental immunology. 2012; 2012:467154. [PubMed: 22489249]

Alirezaei M, Kiosses WB, Flynn CT, Brady NR, Fox HS. Disruption of neuronal autophagy by infected microglia results in neurodegeneration. PloS one. 2008; 3:e2906. [PubMed: 18682838]

Atluri VS, Hidalgo M, Samikkannu T, Kurapati KR, Jayant RD, Sagar V, Nair MP. Effect of human immunodeficiency virus on blood-brain barrier integrity and function: an update. Frontiers in cellular neuroscience. 2015; 9:212. [PubMed: 26113810]

Begley DJ. Delivery of therapeutic agents to the central nervous system: the problems and the possibilities. Pharmacology & therapeutics. 2004; 104:29–45. [PubMed: 15500907]

Bennasser Y, Yeung ML, Jeang KT. RNAi therapy for HIV infection: principles and practicalities. BioDrugs: clinical immunotherapeutics, biopharmaceuticals and gene therapy. 2007; 21:17–22.

Chaudhuri A, Yang B, Gendelman HE, Persidsky Y, Kanmogne GD. STAT1 signaling modulates HIV-1-induced inflammatory responses and leukocyte transmigration across the blood-brain barrier. Blood. 2008; 111:2062–2072. [PubMed: 18003888]

Cheng-Mayer C, Levy JA. Distinct biological and serological properties of human immunodeficiency viruses from the brain. Annals of neurology. 1988; 23(Suppl):S58–61. [PubMed: 3258140]

Churchill MJ, Figueiredo A, Cowley D, Gray L, Purcell DF, Sullivan JS, McPhee DA, Wesselingh SL, Brew BJ, Gorry PR. Transcriptional activity of blood-and cerebrospinal fluid-derived nef/long-terminal repeat sequences isolated from a slow progressor infected with nef-deleted human immunodeficiency virus type 1 (HIV-1) who developed HIV-associated dementia. Journal of neurovirology. 2006; 12:219–228. [PubMed: 16877303]

Criollo A, Senovilla L, Authier H, Maiuri MC, Morselli E, Vitale I, Kepp O, Tasdemir E, Galluzzi L, Shen S, Tailler M, Delahaye N, Tesniere A, De Stefano D, Younes AB, Harper F, Pierron G, Lavandero S, Zitvogel L, Israel A, Baud V, Kroemer G. The IKK complex contributes to the induction of autophagy. The EMBO journal. 2010; 29:619–631. [PubMed: 19959994]

Dahal S, Chitti SV, Nair MP, Saxena SK. Interactive effects of cocaine on HIV infection: implication in HIV-associated neurocognitive disorder and neuroAIDS. Frontiers in microbiology. 2015; 6:931. [PubMed: 26441868]

Deretic V, Saitoh T, Akira S. Autophagy in infection, inflammation and immunity. Nature reviews Immunology. 2013; 13:722–737.

Dinkins C, Pilli M, Kehrl JH. Roles of autophagy in HIV infection. Immunology and cell biology. 2015; 93:11–17. [PubMed: 25385065]

El-Hage N, Bruce-Keller AJ, Knapp PE, Hauser KF. CCL5/RANTES gene deletion attenuates opioid-induced increases in glial CCL2/MCP-1 immunoreactivity and activation in HIV-1 Tat-exposed mice. Journal of neuroimmune pharmacology: the official journal of the Society on NeuroImmune Pharmacology. 2008; 3:275–285. [PubMed: 18815890]

El-Hage N, Dever SM, Podhaizer EM, Arnatt CK, Zhang Y, Hauser KF. A novel bivalent HIV-1 entry inhibitor reveals fundamental differences in CCR5-mu-opioid receptor interactions between human astroglia and microglia. AIDS (London, England). 2013; 27:2181–2190.

El-Hage N, Rodriguez M, Dever SM, Masvekar RR, Gewirtz DA, Shacka JJ. HIV-1 and morphine regulation of autophagy in microglia: limited interactions in the context of HIV-1 infection and opioid abuse. Journal of virology. 2015; 89:1024–1035. [PubMed: 25355898]

El-Hage N, Rodriguez M, Podhaizer EM, Zou S, Dever SM, Snider SE, Knapp PE, Beardsley PM, Hauser KF. Ibudilast (AV411), and its AV1013 analog, reduce HIV-1 replication and neuronal death induced by HIV-1 and morphine. AIDS (London, England). 2014

Ene L, Duiculescu D, Ruta SM. How much do antiretroviral drugs penetrate into the central nervous system? Journal of medicine and life. 2011; 4:432–439. [PubMed: 22514580]

Eskelinen EL. Doctor Jekyll and Mister Hyde: autophagy can promote both cell survival and cell death. Cell death and differentiation. 2005; 12(Suppl 2):1468–1472. [PubMed: 16247492]

Eugenin EA, Osiecki K, Lopez L, Goldstein H, Calderon TM, Berman JW. CCL2/monocyte chemoattractant protein-1 mediates enhanced transmigration of human immunodeficiency virus (HIV)-infected leukocytes across the blood-brain barrier: a potential mechanism of HIV-CNS invasion and NeuroAIDS. The Journal of neuroscience: the official journal of the Society for Neuroscience. 2006; 26:1098–1106. [PubMed: 16436595]

Fan J, Nishanian P, Breen EC, McDonald M, Fahey JL. Cytokine gene expression in normal human lymphocytes in response to stimulation. Clinical and diagnostic laboratory immunology. 1998; 5:335–340. [PubMed: 9605988]

Fiandra L, Colombo M, Mazzucchelli S, Truffi M, Santini B, Allevi R, Nebuloni M, Capetti A, Rizzardini G, Prosperi D, Corsi F. Nanoformulation of antiretroviral drugs enhances their penetration across the blood brain barrier in mice. Nanomedicine: nanotechnology, biology, and medicine. 2015; 11:1387–1397.

Fields J, Dumaop W, Rockenstein E, Mante M, Spencer B, Grant I, Ellis R, Letendre S, Patrick C, Adame A, Masliah E. Age-dependent molecular alterations in the autophagy pathway in HIVE patients and in a gp120 tg mouse model: reversal with beclin-1 gene transfer. Journal of neurovirology. 2013; 19:89–101. [PubMed: 23341224]

Fiume G, Vecchio E, De Laurentiis A, Trimboli F, Palmieri C, Pisano A, Falcone C, Pontoriero M, Rossi A, Scialdone A, Fasanella Masci F, Scala G, Quinto I. Human immunodeficiency virus-1 Tat activates NF-kappaB via physical interaction with IkappaB-alpha and p65. Nucleic acids research. 2012; 40:3548–3562. [PubMed: 22187158]

Fu LL, Cheng Y, Liu B. Beclin-1: autophagic regulator and therapeutic target in cancer. The international journal of biochemistry & cell biology. 2013; 45:921–924. [PubMed: 23420005]

Graziosi C, Gantt KR, Vaccarezza M, Demarest JF, Daucher M, Saag MS, Shaw GM, Quinn TC, Cohen OJ, Welbon CC, Pantaleo G, Fauci AS. Kinetics of cytokine expression during primary human immunodeficiency virus type 1 infection. Proceedings of the National Academy of Sciences of the United States of America. 1996; 93:4386–4391. [PubMed: 8633076]

Guo ML, Liao K, Periyasamy P, Yang L, Cai Y, Callen SE, Buch S. Cocaine-mediated microglial activation involves the ER stress-autophagy axis. Autophagy. 2015; 11:995–1009. [PubMed: 26043790]

Hazleton JE, Berman JW, Eugenin EA. Novel mechanisms of central nervous system damage in HIV infection. HIV/AIDS (Auckland, NZ). 2010; 2:39–49.

He C, Levine B. The Beclin 1 interactome. Current opinion in cell biology. 2010; 22:140–149. [PubMed: 20097051]

Heaton RK, Franklin DR, Ellis RJ, McCutchan JA, Letendre SL, Leblanc S, Corkran SH, Duarte NA, Clifford DB, Woods SP, Collier AC, Marra CM, Morgello S, Mindt MR, Taylor MJ, Marcotte TD, Atkinson JH, Wolfson T, Gelman BB, McArthur JC, Simpson DM, Abramson I, Gamst A, Fennema-Notestine C, Jernigan TL, Wong J, Grant I, Group C, Group H. HIV-associated neurocognitive disorders before and during the era of combination antiretroviral therapy: differences in rates, nature, and predictors. Journal of neurovirology. 2011; 17:3–16. [PubMed: 21174240]

Jayant RD, Atluri VS, Agudelo M, Sagar V, Kaushik A, Nair M. Sustained-release nanoART formulation for the treatment of neuroAIDS. International journal of nanomedicine. 2015; 10:1077–1093. [PubMed: 25709433]

Jiang Y, Zhu J, Wu L, Xu G, Dai J, Liu X. Tetracycline inhibits local inflammation induced by cerebral ischemia via modulating autophagy. PloS one. 2012; 7:e48672. [PubMed: 23144925]

Juliano RL, Alahari S, Yoo H, Kole R, Cho M. Antisense pharmacodynamics: critical issues in the transport and delivery of antisense oligonucleotides. Pharmaceutical research. 1999; 16:494–502. [PubMed: 10227702]

Kang R, Zeh HJ, Lotze MT, Tang D. The Beclin 1 network regulates autophagy and apoptosis. Cell death and differentiation. 2011; 18:571–580. [PubMed: 21311563]

Kaul M, Garden GA, Lipton SA. Pathways to neuronal injury and apoptosis in HIV-associated dementia. Nature. 2001; 410:988–994. [PubMed: 11309629]

Kaushik A, Jayant RD, Nikkhah-Moshaie R, Bhardwaj V, Roy U, Huang Z, Ruiz A, Yndart A, Atluri V, El-Hage N, Khalili K, Nair M. Magnetically guided central nervous system delivery and toxicity evaluation of magneto-electric nanocarriers. Scientific Reports. 2016; 6:25309. [PubMed: 27143580]

Kumar A, Singh UK, Chaudhary A. Targeting autophagy to overcome drug resistance in cancer therapy. Future medicinal chemistry. 2015; 7:1535–1542. [PubMed: 26334206]

Kumar P, Ban HS, Kim SS, Wu H, Pearson T, Greiner DL, Laouar A, Yao J, Haridas V, Habiro K, Yang YG, Jeong JH, Lee KY, Kim YH, Kim SW, Peipp M, Fey GH, Manjunath N, Shultz LD, Lee SK, Shankar P. T cell-specific siRNA delivery suppresses HIV-1 infection in humanized mice. Cell. 2008; 134:577–586. [PubMed: 18691745]

Lamers SL, Salemi M, Galligan DC, Morris A, Gray R, Fogel G, Zhao L, McGrath MS. Human immunodeficiency virus-1 evolutionary patterns associated with pathogenic processes in the brain. Journal of neurovirology. 2010; 16:230–241. [PubMed: 20367240]

Lee SK, Dykxhoorn DM, Kumar P, Ranjbar S, Song E, Maliszewski LE, Francois-Bongarcon V, Goldfeld A, Swamy NM, Lieberman J, Shankar P. Lentiviral delivery of short hairpin RNAs protects CD4 T cells from multiple clades and primary isolates of HIV. Blood. 2005; 106:818–826. [PubMed: 15831707]

Liu Y, Levine B. Autosis and autophagic cell death: the dark side of autophagy. Cell death and differentiation. 2015; 22:367–376. [PubMed: 25257169]

McKnight NC, Zhenyu Y. Beclin 1, an Essential Component and Master Regulator of PI3K-III in Health and Disease. Current pathobiology reports. 2013; 1:231–238. [PubMed: 24729948]

Minogue AM, Barrett JP, Lynch MA. LPS-induced release of IL-6 from glia modulates production of IL-1beta in a JAK2-dependent manner. Journal of neuroinflammation. 2012; 9:126. [PubMed: 22697788]

Mizushima N, Yoshimori T, Levine B. Methods in mammalian autophagy research. Cell. 2010; 140:313–326. [PubMed: 20144757]

Nair M, Guduru R, Liang P, Hong J, Sagar V, Khizroev S. Externally controlled on-demand release of anti-HIV drug using magneto-electric nanoparticles as carriers. Nature communications. 2013; 4:1707.

Nath A, Steiner J. Synaptodendritic injury with HIV-Tat protein: What is the therapeutic target? Experimental neurology. 2014; 251:112–114. [PubMed: 24246278]

Neun BW, Stern ST. Monitoring lysosomal activity in nanoparticle-treated cells. Methods in molecular biology (Clifton, NJ). 2011; 697:207–212.

Nolting T, Lindecke A, Koutsilieri E, Maschke M, Husstedt IW, Sopper S, Stuve O, Hartung HP, Arendt G. Measurement of soluble inflammatory mediators in cerebrospinal fluid of human immunodeficiency virus-positive patients at distinct stages of infection by solid-phase protein array. Journal of neurovirology. 2009; 15:390–400. [PubMed: 20001608]

Novina CD, Murray MF, Dykxhoorn DM, Beresford PJ, Riess J, Lee SK, Collman RG, Lieberman J, Shankar P, Sharp PA. siRNA-directed inhibition of HIV-1 infection. Nature medicine. 2002; 8:681–686.

Pardridge WM. shRNA and siRNA delivery to the brain. Advanced drug delivery reviews. 2007; 59:141–152. [PubMed: 17434235]

Park HY, Kim TH, Kim CG, Kim GY, Kim CM, Kim ND, Kim BW, Hwang HJ, Choi YH. Purpurogallin exerts antiinflammatory effects in lipopolysaccharidestimulated BV2 microglial cells through the inactivation of the NFkappaB and MAPK signaling pathways. International journal of molecular medicine. 2013; 32:1171–1178. [PubMed: 24002379]

Parzych KR, Klionsky DJ. An overview of autophagy: morphology, mechanism, and regulation. Antioxidants & redox signaling. 2014; 20:460–473. [PubMed: 23725295]

Pitha PM. Innate antiviral response: role in HIV-1 infection. Viruses. 2011; 3:1179–1203. [PubMed: 21994776]

Qing G, Yan P, Qu Z, Liu H, Xiao G. Hsp90 regulates processing of NF-kappa B2 p100 involving protection of NF-kappa B-inducing kinase (NIK) from autophagy-mediated degradation. Cell research. 2007; 17:520–530. [PubMed: 17563756]

Rossi JJ. RNAi therapeutics: SNALPing siRNAs in vivo. Gene therapy. 2006; 13:583–584. [PubMed: 17526070]

Ryther RC, Flynt AS, Phillips JA 3rd, Patton JG. siRNA therapeutics: big potential from small RNAs. Gene therapy. 2005; 12:5–11. [PubMed: 15496962]

Shpilka T, Weidberg H, Pietrokovski S, Elazar Z. Atg8: an autophagy-related ubiquitin-like protein family. Genome biology. 2011; 12:226. [PubMed: 21867568]

Stern ST, Adiseshaiah PP, Crist RM. Autophagy and lysosomal dysfunction as emerging mechanisms of nanomaterial toxicity. Particle and fibre toxicology. 2012; 9:20. [PubMed: 22697169]

Stern ST, Johnson DN. Role for nanomaterial-autophagy interaction in neurodegenerative disease. Autophagy. 2008; 4:1097–1100. [PubMed: 18927490]

Sun L, Liu N, Liu SS, Xia WY, Liu MY, Li LF, Gao JX. Beclin-1-independent autophagy mediates programmed cancer cell death through interplays with endoplasmic reticulum and/or mitochondria in colbat chloride-induced hypoxia. American journal of cancer research. 2015; 5:2626–2642. [PubMed: 26609472]

Suri SS, Fenniri H, Singh B. Nanotechnology-based drug delivery systems. Journal of occupational medicine and toxicology (London, England). 2007; 2:16.

Wang S, Wang H, Jing H, Wang S, Kang L, Gao X, Hu L, Zheng X. Anti-inflammatory effects of isopropyl 3-(3, 4-dihydroxyphenyl)-2-hydroxypropanoate, a novel metabolite from danshen, on activated microglia. The Chinese journal of physiology. 2012; 55:428–434. [PubMed: 23286451]

Wang Z, Pekarskaya O, Bencheikh M, Chao W, Gelbard HA, Ghorpade A, Rothstein JD, Volsky DJ. Reduced expression of glutamate transporter EAAT2 and impaired glutamate transport in human primary astrocytes exposed to HIV-1 or gp120. Virology. 2003; 312:60–73. [PubMed: 12890621]

Wohlfart S, Gelperina S, Kreuter J. Transport of drugs across the blood-brain barrier by nanoparticles. Journal of controlled release: official journal of the Controlled Release Society. 2012; 161:264–273. [PubMed: 21872624]

Wu H, Zhang HJ, Zhang XM, Xu HF, Wang M, Huang JD, Zheng BJ. Identification of drug resistant mutations in HIV-1 CRF07_BC variants selected by nevirapine in vitro. PloS one. 2012; 7:e44333. [PubMed: 22984494]

Yang B, Akhter S, Chaudhuri A, Kanmogne GD. HIV-1 gp120 induces cytokine expression, leukocyte adhesion, and transmigration across the blood-brain barrier: modulatory effects of STAT1 signaling. Microvascular research. 2009; 77:212–219. [PubMed: 19103208]

Yue Z, Jin S, Yang C, Levine AJ, Heintz N. Beclin 1, an autophagy gene essential for early embryonic development, is a haploinsufficient tumor suppressor. Proceedings of the National Academy of Sciences of the United States of America. 2003; 100:15077–15082. [PubMed: 14657337]
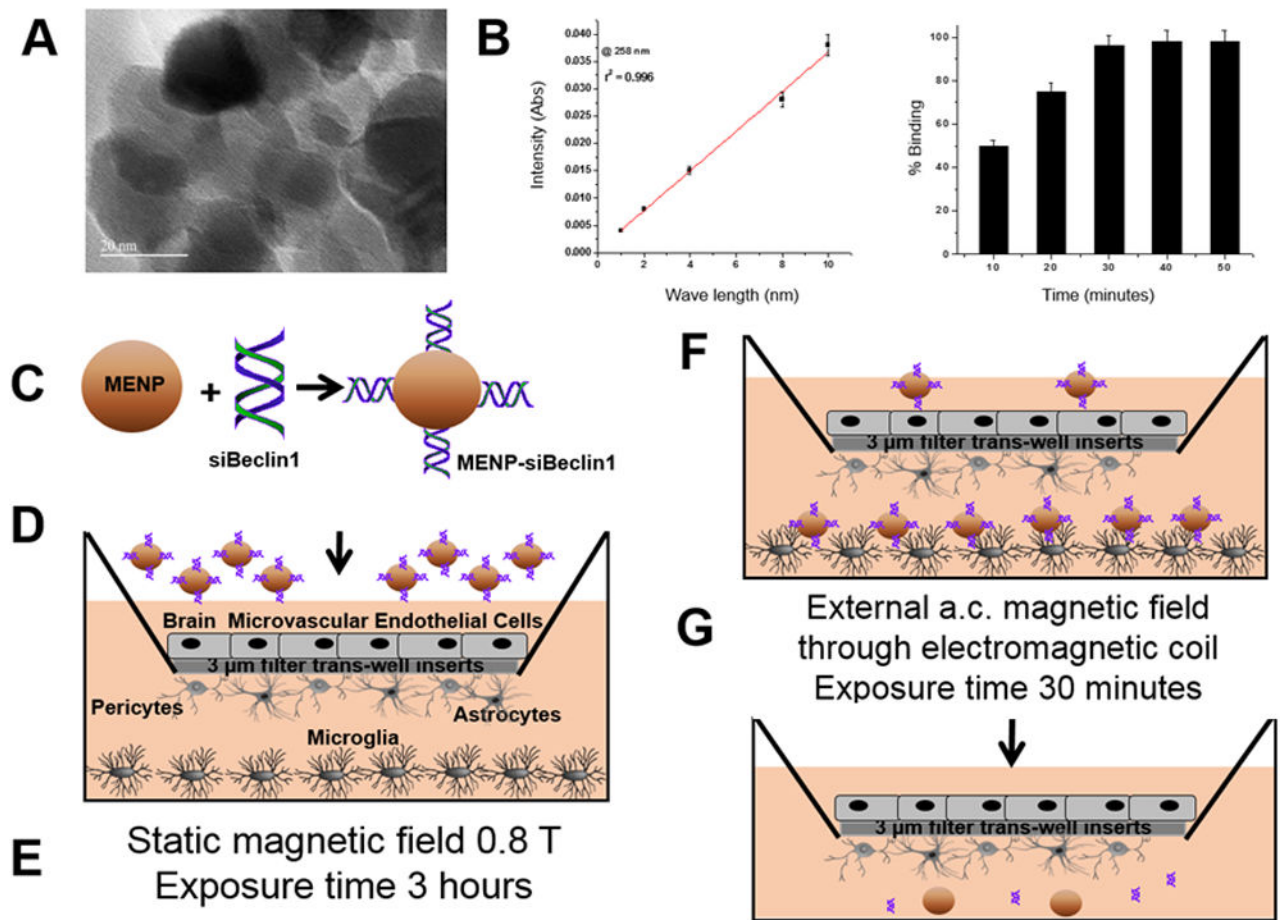
Figure 1. Nano-bound siRNA-Beclin1 crosses artificial blood brain barrier
Transmission electron microscopy (TEM) of MENP collected from the bottom chamber of
the BBB after 24 hours post-treatment (A). Standard curve and time kinetics of siBeclin1
binding to magneto-electric nanoparticles (MENPs) showing binding efficiencies as a matter
of time (B). Schematic representation of the nano-formulation design (C). Schematic
representation of the artificial blood brain barrier (BBB) and structural detailed of brain cell
types involved. BBB was used to measure transmigration of nano-formulation and efficacy
of siBeclin1 in viral-infected cells. (D). Plate was placed for 3 hours under a magnetic field
(0.8 Tesla) to drive the nano-formulation across the BBB (E–F). External a.c. magnetic field
was applied for 30 minutes to releases the siRNA (G).
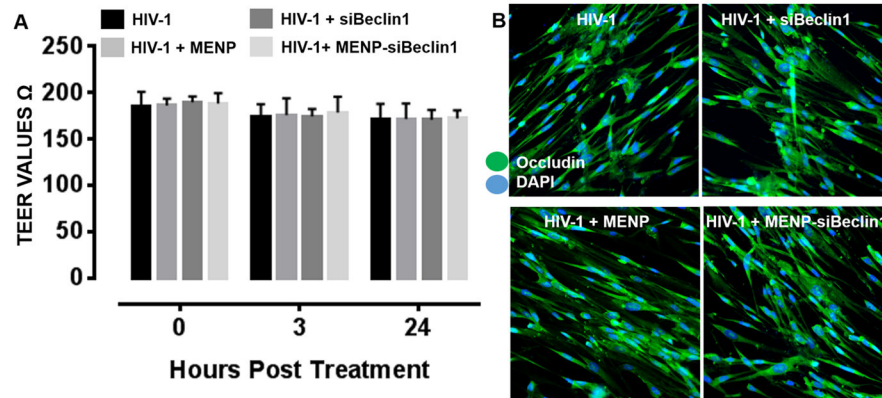
Figure 2. Nano-bound Beclin1 siRNA does not compromise the physiological function of the artificial blood brain barrier

Transendothelial electrical resistance (TEER) across the brain microvascular endothelial cell monolayer of the BBB model was measured following the indicated treatments at the indicated time points. Error bars show the SEM for 3 independent experiments (A). Expression of occludin protein was detected in brain microvascular endothelial cells by immunocytochemistry following the indicated treatments for 24 hours. Cells were immunolabeled with an antibody to occludin (*green*) and DAPI (*blue*) staining was used to label cell nuclei. Representative images were acquired at 20X magnification (B).
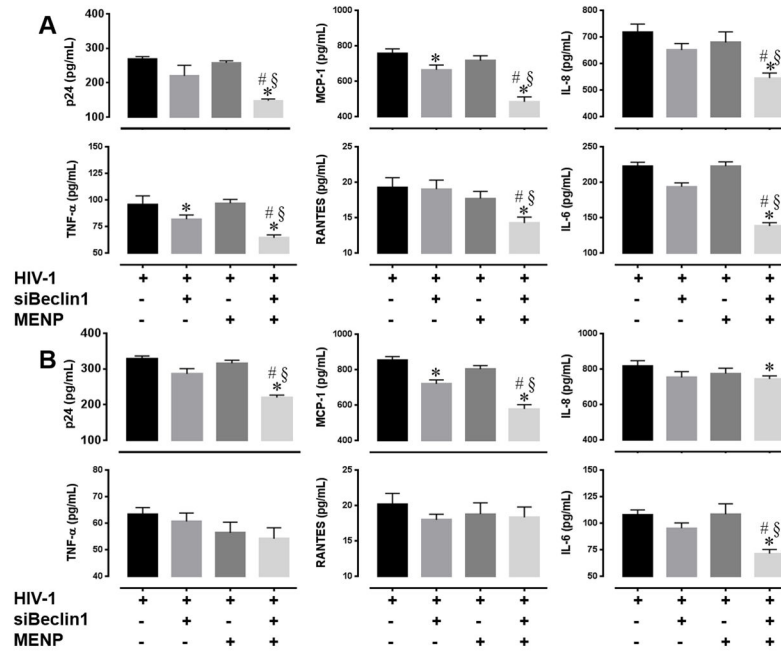
Figure 3. Nano-bound Beclin1 siRNA attenuates viral replication and HIV-induced inflammation in microglia cells

HIV-1 p24 protein levels and the indicated cytokines and chemokines in microglial supernatants were measured by ELISA after (A) 24 and (B) 48 hours following the indicated treatments. Error bars show the SEM for 3 independent experiments. P<0.05* vs. HIV-1; # vs. HIV-1 + MENP; § vs. HIV-1 + siBeclin1.
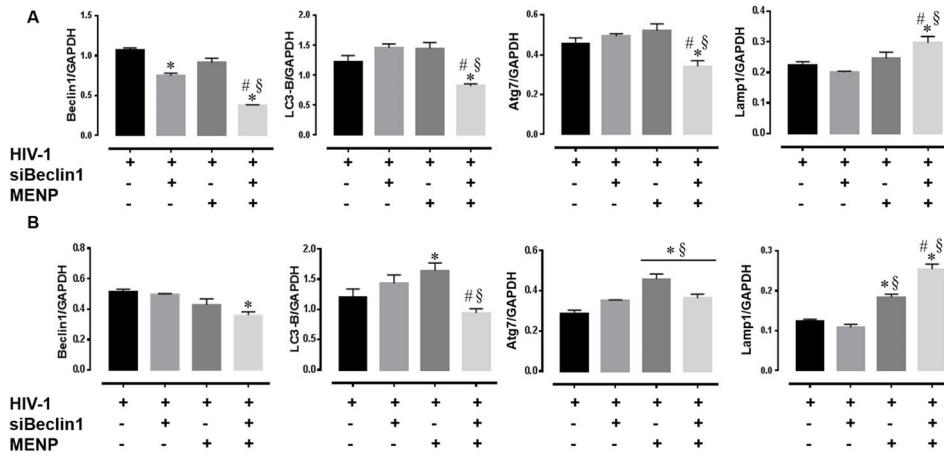
Figure 4. Nano-bound Beclin1 siRNA crosses artificial blood brain barrier and silences Beclin1 protein expression levels in microglia

Microglial whole cell lysates were analyzed by Western blotting for the indicated proteins after (A) 24 and (B) 48 hours following the indicated treatments. Protein levels of interest were normalized to GAPDH. Error bars show the SEM for 3 independent experiments. P<0.05* vs. HIV-1; # vs. HIV-1 + MENP; § vs. HIV-1 + siBeclin1.
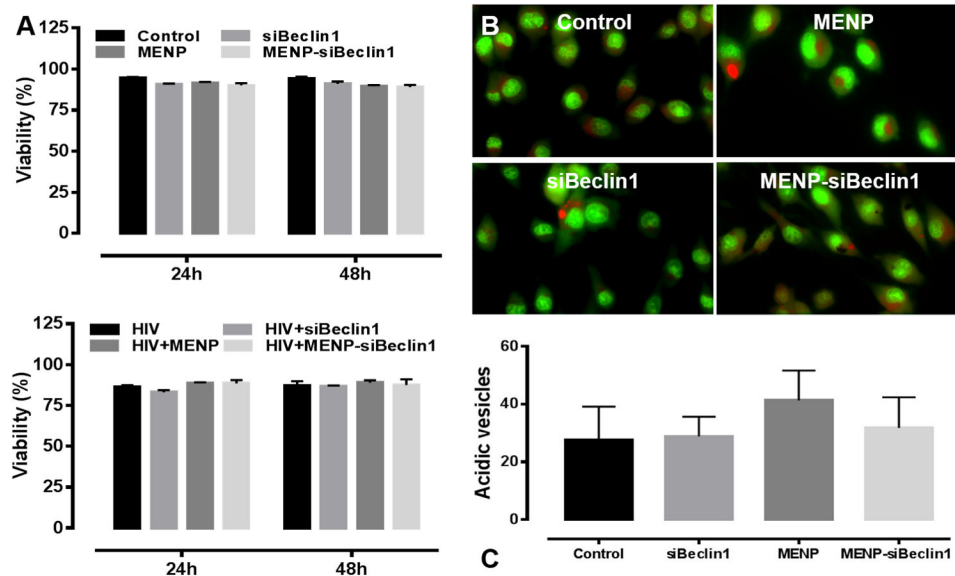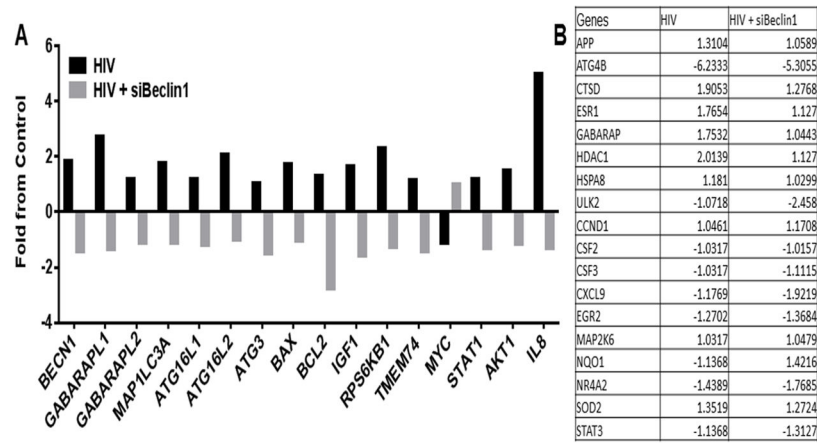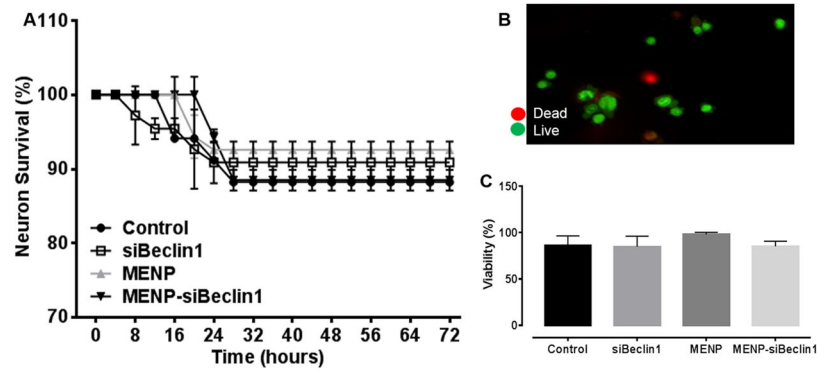
Figure 5. Nano-bound Beclin1 siRNA does not compromise microglia viability
Viability of microglia was assessed following the indicated treatments at the indicated time points using a live/dead cell fluorescence assay. Error bars show the SEM for 3 independent experiments with at least 50 cells per experiment (A). Cellular pH in microglia was assessed following the indicated treatments for 24 hours using acridine orange (AO) staining. Under acidic conditions, AO-stained cells fluoresce bright *red*, whereas basic environments such as the cytoplasm and nucleolus fluoresce bright *green* and dim *red*. Representative images were acquired at 63X magnification (B). Quantification of acidic (*red*) vesicles from panel (B). Error bars show the SEM for 3 independent experiments with at least 25 cells per experiment (C).

Genes	HIV	HIV + siBeclin1
APP	1.3104	1.0589
ATG4B	-6.2333	-5.3055
CTSD	1.9053	1.2768
ESR1	1.7654	1.127
GABARAP	1.7532	1.0443
HDAC1	2.0139	1.127
HSPA8	1.181	1.0299
ULK2	-1.0718	-2.458
CCND1	1.0461	1.1708
CSF2	-1.0317	-1.0157
CSF3	-1.0317	-1.1115
CXCL9	-1.1769	-1.9219
EGR2	-1.2702	-1.3684
MAP2K6	1.0317	1.0479
NQO1	-1.1368	1.4216
NR4A2	-1.4389	-1.7685
SOD2	1.3519	1.2724
STAT3	-1.1368	-1.3127

Figure 6. Epigenetics studies using RNA from HIV-infected microglial cell ± siBeclin1
Relative mRNA expression of the indicated genes was measured using NF-κB-mediated signal transduction and autophagy PCR arrays following the indicated treatments for 24 hours (A). Expression of genes not affected by siBeclin1 (B). Data represent the combined analysis of three independent experiments.

Figure 7. Nano-bound Beclin1 siRNA does not compromise neuronal viability
Individual neurons were scored for survival using time-lapse imaging at the indicated time points following the indicated treatments. Error bars show the SEM for 2 independent experiments with at least 50 cells per experiment (A). Neuronal viability was confirmed using a live/dead cell fluorescence assay (B–C). A representative image of dead (*red*) and live (*green*) cells acquired at 20X magnification is shown (B). Viability was manually quantified following the indicated treatments for 72 hours. Error bars show the SEM for 3 independent experiments with at least 50 cells per experiment (C).